Climate of the Past
Open Access
Discussions

Freshwater discharge controlled deposition of Cenomanian-Turonian black shales on the NW European epicontinental shelf (Wunstorf, North Germany)

N. A. G. M. van Helmond[1], A. Sluijs[1], J. S. Sinninghe Damsté[2,3], G.-J. Reichart[2,3], S. Voigt[4], J. Erbacher[5], J. Pross[6], and H. Brinkhuis[1,3]

[1]Marine Palynology and Paleoceanography, Laboratory of Palaeobotany and Palynology, Department of Earth Sciences, Faculty of Geosciences, Utrecht University., Budapestlaan 4, 3584 CD Utrecht, the Netherlands
[2]Department of Earth Sciences, Faculty of Geosciences, Utrecht University, Budapestlaan 4, 3584 CD Utrecht, the Netherlands
[3]NIOZ, Royal Netherlands Institute for Sea Research, P.O. Box 59, 1790 AB Den Burg, Texel, the Netherlands
[4]Institute of Geosciences, Goethe-University Frankfurt, Altenhöferallee 1, 60438 Frankfurt, Germany

CPD

10, 3755–3786, 2014

Freshwater forced black shale deposition during OAE2

N. A. G. M. van Helmond et al.

Title Page

Abstract	Introduction
Conclusions	References
Tables	Figures

|◀ | ▶|
◀ | ▶

Back | Close

Full Screen / Esc

Printer-friendly Version

Interactive Discussion

[5]Bundesanstalt für Geowissenschaften und Rohstoffe, P.O. Box 51 01 53, Alfred-Benz-Haus, Stilleweg 2, 30641 Hanover, Germany

[6]Paleoenvironmental Dynamics Group, Institute of Earth Sciences, University of Heidelberg, Im Neuenheimer Feld 234, 69120 Heidelberg, Germany

Correspondence to: N. A. G. M. van Helmond (n.vanhelmond@uu.nl)

CPD

10, 3755–3786, 2014

Freshwater forced black shale deposition during OAE2

N. A. G. M. van Helmond et al.

Title Page

Abstract	Introduction
Conclusions	References
Tables	Figures

|◄ | ►|

◄ | ►

Back | Close

Full Screen / Esc

Printer-friendly Version

Interactive Discussion

N. A. G. M. van Helmond et al.

Abstract

Global warming, changes in the hydrological cycle and enhanced marine primary productivity all have been invoked to have contributed to the occurrence of widespread ocean anoxia during the Cenomanian-Turonian Oceanic Anoxic Event (OAE2; $\sim$ 94 Ma), but disentangling these factors on a regional scale has remained problematic. We generated palynological and organic geochemical records that allow the separation of these forcing factors in a core spanning the OAE2 from Wunstorf, Lower Saxony Basin (LSB; North Gemany), which exhibits cyclic black shale–marl alternations related to the orbital precession cycle.

Despite the widely varying depositional conditions complicating the interpretation of the obtained records, TEX_{86}^{H} indicates that sea-surface temperature (SST) evolution in the LSB during OAE2 resembles that of previously studied sites throughout the proto-North Atlantic. Cooling during the so-called Plenus Cold Event interrupted black shale deposition during the early stages of OAE2. However, TEX_{86} does not vary significantly across marl–black shale alternations, suggesting that temperature variations did not force the formation of the cyclic black shale horizons. Relative (i.e., with respect to marine palynomorphs) and absolute abundances of pollen and spores are elevated during phases of black shale deposition, indicative of enhanced precipitation and run-off. High abundances of cysts from inferred heterotrophic and euryhaline dinoflagellates supports high run-off, which likely introduced additional nutrients to the epicontinental shelf resulting in elevated marine primary productivity.

We conclude that orbitally-forced enhanced precipitation and run-off, in tandem with elevated marine primary productivity, were critical in cyclic black shale formation on the northwest European epicontinental shelf and potentially for other OAE2 sections in the proto-Atlantic and Western Interior Seaway at similar latitudes as well.

Freshwater forced black shale deposition during OAE2

N. A. G. M. van Helmond et al.

1   Introduction

Dark, often laminated marine sediments that are usually devoid of fossil traces of benthic life and exhibit a total organic carbon (TOC) content of $> 1\%$ (Creaney and Passey, 1993), were episodically deposited during Jurassic and Cretaceous times. The deposition of these sediments, generally referred to as black shales, has typically been taken to indicate ancient episodes of dys- or anoxic bottom water conditions (Schlanger and Jenkyns, 1976). During some of these episodes, anoxia developed widespread in one or more ocean basins; such episodes were termed Oceanic Anoxic Events (OAEs; Schlanger and Jenkyns, 1976). One of the most prominent, best-constrained and best-studied of these OAEs formed across the Cenomanian–Turonian boundary (CTB; ~ 94 Ma) and became known as OAE2 (e.g. Jenkyns, 2010). The widespread enhanced organic carbon burial in marine sediments during OAE2 is expressed by a worldwide documented $> 2\%$ positive excursion in the carbon isotopic composition of carbonate ($\delta^{13}C_{carb}$) and organic matter ($\delta^{13}C_{org}$), with an estimated duration of 450–600 kyr (e.g. Voigt et al., 2008; Meyers et al., 2012). This excursion likely resulted from enhanced burial of $\delta^{13}C$-depleted organic matter (Arthur et al., 1988; Tsikos et al., 2004) and therefore provides a C-isotopic signature of the global exogenic carbon pool, making it a proper tool to confidently correlate OAE2 sections.

Over the past decades, many studies have been conducted to unravel the processes responsible for this massive burial of organic carbon during OAEs, and OAE2 in particular. Extensive volcanism close to the CTB (e.g. Snow et al., 2005; Kuroda et al., 2007; Turgeon and Craser, 2008) has been linked to high levels of atmospheric CO_2 (e.g. Schouten et al., 2003; Sinninghe Damsté et al., 2008; Barclay et al., 2010), raising the temperatures of already warm oceans towards a maximum at the onset of OAE2 (e.g. Bice et al., 2006; Forster et al., 2007), thereby diminishing oxygen solubility in the surface waters. This warming caused an enhanced hydrological cycle (van Helmond et al., 2014), which would likely have contributed to increased rates of continental weathering and runoff (Blätter et al., 2011; Pogge von Strandmann et al., 2013). This, in turn

would have led to at least seasonal stratification and enhanced nutrient supply to continental margins and epicontinental seas. Extensive volcanism may also have directly contributed to ocean fertilization (Kerr et al., 1998; Snow et al., 2005), while changes in proto-Atlantic circulation may have increased the strength of upwelling (e.g. Poulsen et al., 2001; Junium and Arthur, 2007). Enhanced regeneration of sedimentary phosphorus from dysoxic and anoxic sediments (e.g. Kuypers et al., 2004b; Mort et al., 2007) combined with abundant nitrogen-fixing cyanobacteria (Kuypers et al., 2004b) may have sustained high levels of primary productivity. All of the above factors would conspire to expansion of oxygen minimum zones and oxygen depletion of bottom waters, leading to enhanced organic carbon burial.

As a result of late Cenomanian sea level rise (e.g. Erbacher et al., 1996; Voigt et al., 2006), large parts of continents became flooded, greatly expanding the extent of epicontinental shelf seas where sediments recording the OAE2 were deposited. Particularly the Lower Saxony Basin (LSB; northwest Germany) exhibits expanded and complete OAE2-successions (Wilmsen, 2003) containing several cyclic alternations of organic-poor marls, limestones and organic-rich black shales (Voigt et al., 2008). Organic matter accumulation on the European shelf was relatively modest, however, compared with other cyclic OAE2-sections in the proto-Atlantic (Kuypers et al., 2004a; Forster et al., 2008).

The complete OAE2-interval has been recovered from the LSB through coring at Wunstorf (Erbacher et al., 2007; North Germany; Fig. 1). Application of an orbital cycle-based age model has shown that black shale deposition in the Wunstorf core sediments is consistent with precession forcing (Voigt et al., 2008). This implies that climate change resulting from orbital fluctuations was directly related to phases of black shale deposition. The robust cyclostratigraphy and biostratigraphic zonation of the Wunstorf core allows for a high-resolution study of astronomically-induced climate change. Here we aim to reconstruct mean annual sea surface temperature (SST), hydrological changes and marine primary productivity, to determine the dominant control on decreasing oxygen concentrations during OAE2 on the European shelf. To this end,

Freshwater forced black shale deposition during OAE2

N. A. G. M. van Helmond et al.

Title Page

Abstract	Introduction
Conclusions	References
Tables	Figures

Back | Close

Full Screen / Esc

Printer-friendly Version

Interactive Discussion

we combined organic geochemical (TEX$_{86}$; BIT index) and palynological proxies, notably organic-walled dinoflagellate cysts (dinocysts) and pollen and spore abundances, across the CTB for the Wunstorf core.

2 Material and methods

2.1 Site description, depositional setting and age model

The Wunstorf core was drilled in 2006 $\sim$ 25 km west of Hannover, Germany (TK 25 Wunstorf, no. 3522, 52°23.942′ N, 9°28.824′ E; Fig. 1). Approximately 76 m of middle Cenomanian to middle Turonian sediments, comprising a $\sim$ 13.5 m thick CTB succession, were retrieved. During the Late Cretaceous, the drill site was located in the LSB, which was part of the expanded epicontinental shelf sea that covered most of Eurasia after the Cenomanian transgression (Hancock and Kauffman, 1979). The sediments at Wunstorf were deposited at an estimated water depth of 100–150 m based on sequence stratigraphy, sedimentological analysis and (micro)fossil content (Wilmsen, 2003). The most proximal exposed land, the Rheno-Bohemian Massif, was located $\sim$ 150 km to the south and formed a barrier towards the Western Tethys. The Armorican and British massifs formed a barrier towards the Atlantic, while the Fennoscandian Shield formed a barrier to the open ocean in the north (Fig. 1; Wilmsen, 2003).

The OAE2-interval at Wunstorf is part of the Hesseltal Formation and occurs between 49.6 and 23.1 m below surface (mbs). The Hesseltal Formation consists of rhythmically alternating couplets of finely laminated black shales relatively rich in total organic carbon (TOC; max. 2.8 %; Hetzel et al., 2011; Fig. 2b), grey to green marls, and light-grey (marly) limestones (Fig. 2; Erbacher et al., 2007; Voigt et al., 2008). The cyclic lithology results from a depositional system greatly influenced by precession (Voigt et al., 2008). Biostratigraphic zonation for the Hesseltal Formation relies on inoceramids, ammonites, acme occurrences of macrofossils and planktonic foraminifera

Freshwater forced black shale deposition during OAE2

N. A. G. M. van Helmond et al.

that can be reliably correlated regionally and globally (Ernst et al., 1984; Voigt et al., 2008, and references therein).

The onset of the OAE2-interval is primarily based on the first occurrence (FO) of the ammonite *Metoicoceras geslinianum* at 49.6 mbs, consistent with the English Chalk (Voigt et al., 2008). At 47.8 mbs, the onset of the characteristic positive shift in $\delta^{13}C_{carb}$ (∼ 2‰) and $\delta^{13}C_{org}$ (∼ 2.5‰) was recognized (Voigt et al., 2008; Du Vivier et al., 2014; Fig. 2a). The termination of the OAE2 interval at Wunstorf was placed at 36 mbs (Voigt et al., 2008). The duration of the OAE2 for the Wunstorf core was estimated at ∼ 435 kyr or ∼ 500 kyr based on spectral analyses of the lithological cyclicity and $\delta^{13}C_{org}$, respectively (Voigt et al., 2008; Du Vivier et al., 2014).

2.2 Total organic carbon analysis

About 0.3 g of freeze-dried and powdered sediment sample was decalcified using 1 M HCl, followed by rinsing with demineralized water and drying again. Total Organic Carbon (TOC) concentrations were measured using a Fisons Instruments CNS NA 1500 analyzer and corrected for weight loss during decalcification. Results were normalized to in-house standards, acetanilide, atropine and nicotinamide. The average analytical uncertainty based on duplicate analyses of sediment samples was 0.04 weight percent (wt.%).

2.3 Organic geochemistry

For 48 samples, organic molecules were extracted from 10–15 g of powdered and freeze-dried sediments with a Dionex accelerated solvent extractor (ASE) using dichloromethane (DCM)/methanol mixture (9 : 1, v/v). Total lipid extracts (TLEs) were evaporated to near dryness using rotary evaporation. Subsequently, remaining solvents were removed under a nitrogen flow. The TLEs were separated by Al_2O_3 column chromatography, into apolar, ketone, glycerol dialkyl glycerol tetraether (GDGT) and polar fractions using the eluents hexane/DCM (9 : 1, v/v), ethyl acetate (v), DCM/methanol

Freshwater forced black shale deposition during OAE2

N. A. G. M. van Helmond et al.

(95 : 5, v/v) and DCM/methanol (1 : 1, v/v), respectively. The apolar and GDGT fractions were dried under a nitrogen flow and weighed. Selected apolar fractions were measured using gas chromatography-mass spectrometry (GC–MS), to determine the thermal maturity of the sediments based on the degree of isomerisation of hopanes. Analyses were performed on a Thermo Finnigan Trace Gas Chromatograph (GC) Ultra connected to a Thermofinnigan DSQ mass spectrometer operated at 70 eV, with a range of m/z 50–800 and a cycle time of 3 scans s^{-1}. The temperature program and column conditions resemble that of Sinninghe Damsté et al. (2008). To quantify the GDGT abundances a known amount of C$_{46}$ GDGT-standard was added (Huguet et al., 2006), after which the GDGT-fractions were re-dissolved in hexane/propanol (99 : 1, v/v) and filtered over a 0.45 μm mesh PTFE filter. The filtered GDGT fractions were analysed using high performance liquid chromatography-atmospheric pressure chemical ionization/mass spectrometry (HPLC-APCI/MS) according to the method described in Schouten et al. (2007). Analysis were performed on an Agilent 1290 infinity series coupled to a 6130 single quadrupole MSD, equipped with auto-injection system and HP-Chemstation software. Separation was achieved on a Prevail Cyano column (150 mm × 2.1 mm, 3 μm; Alltech). Selective ion monitoring was used to detect the GDGTs, for which it was exhibited that for samples with a high TEX$_{86}$ value, a concentration of 0.1 ng of injected GDGTs on the LC column was still sufficient to yield trustworthy TEX$_{86}$ values (Schouten et al., 2007). The minimum GDGT concentration injected on the LC column per measurement in this study was ∼ 0.3 ng. TEX$_{86}$-index values were calculated after Schouten et al. (2002), and converted to absolute annual average sea surface temperatures (SSTs) using the TEX$_{86}^{H}$ Kim et al. (2010) modern core top calibration, which has a calibration error of 2.5 °C. Analytical reproducibility was generally better than 0.3 °C.

The Branched and Isoprenoid Tetraether (BIT) index was used to estimate the relative abundance of soil organic matter in marine sediments (Hopmans et al., 2004). The BIT index is based on the amount of predominantly soil-derived branched GDGTs

(brGDGTs) relative to the isoprenoid GDGT (iGDGT) crenarchaeol, which is chiefly derived from marine Thaumarchaeota.

2.4 Palynology

In total 51 samples were prepared for quantitative palynological analysis. In general between 5 and 10 g, and for samples low in organic carbon up to ~ 20 g, of freeze-dried sediment sample were crushed to pieces smaller than 5 mm. Subsequently a known amount of *Lycopodium* marker spores was added to allow for quantitative analysis. After reaction with ~ 30 % HCl and twice with ~ 38 % HF, to dissolve carbonates and silicates respectively, ultrasonic separation was employed. Finally, samples were sieved over a 15 µm nylon mesh. Residuals were mounted on slides for microscopic analysis. Approximately 250 dinocysts per sample were counted using a light microscope at 500x magnification. Taxonomy follows that of Fensome and Williams (2004). Pollen and spores were counted as one group, except for saccate gymnosperm pollen. All samples and slides are stored in the collection of the Laboratory of Palaeobotany and Palynology, Utrecht University, the Netherlands.

3 Results

3.1 Total organic carbon

Trends in, and absolute values of, TOC (Fig. 2) are generally in agreement with results reported by Hetzel et al. (2011), i.e., relatively high for black shales and low for marls and limestones. The background TOC content is < 0.3 %, somewhat higher than reported by Hetzel et al. (2011). Within the OAE2, four intervals with elevated TOC content are identified. The first interval is between 49 and 47.5 m and contains the first black shale, at the onset of the CIE. A second organic-rich cluster is recognized between ~ 44 and 42 mbs, with the maximum TOC content approaching 2 %. The third organic-rich interval is from 41 to 39.5 mbs, with a maximum TOC content just over

2.5 %. The last organic-rich cluster ranges from 37.5 to 35.5 mbs, with a maximum TOC content just above 2 %. For the remainder of the record, only the youngest sample (26.51 mbs) has an elevated TOC content (close to 1.5 %).

3.2 Thermal maturity

For the selected samples the hopane distribution was determined. $C_{31}17\beta,21\beta$ (H) hopane was the dominant hopane. No $\alpha\beta$-hopanes were encountered, so the ($\beta\beta/(\beta\beta + \beta\alpha + \alpha\alpha)$)) of hopane biomarkers was 1, in agreement with results on sediments from this core presented by Blumenberg and Wiese (2012). This indicates that the thermal maturity of the sedimentary organic matter was sufficiently low for the application of TEX_{86} paleothermometry (Schouten et al., 2004).

3.3 GDGT-based proxies

Except for Sample 41.45 mbs, all samples yielded quantifiable GDGT abundances, although with orders of magnitude differences in concentration (Fig. 2c). Total GDGT concentrations are in the range of 0.13–43 µg g^{-1} organic carbon (OC). Crenarchaeol concentrations vary by three orders of magnitude, whereas brGDGT concentrations vary by one to two orders of magnitude. High GDGT concentrations coincide with the organic carbon-rich black shales (Fig. 2b and c), while low GDGT concentrations coincide with organic-poor sediments (Fig. 2b and c). Values for the BIT-index range from 0.02, indicating low relative abundances of soil-derived brGDGTs, to 0.56, evidencing substantial soil-derived input of brGDGTs. The BIT-index (Fig. 2d) is relatively high in the organic-poor intervals and generally low (i.e. < 0.10) for the organic-rich black-shale intervals. Values for TEX_{86} fluctuate between 0.71 and 0.99 (Fig. 2e).

3.4 Palynology

Nine samples were barren of palynomorphs (Fig. 3c). For the remaining 42 samples, dinocyst concentrations range from ∼ 35 to 15 000 cysts per gram, and pollen and

N. A. G. M. van Helmond et al.

spores concentrations range from 10> to 5000 grains per gram, with highest concentrations in the organic-rich black shales (Fig. 3c).

Palynological assemblages are dominated by dinocysts, ~ 85 % on average (max. > 99 %). Summed pollen and spores, and hence the terrestrially derived fraction, comprises on average ~ 15 % of the assemblage (max. ~ 40 %). The terrestrial over marine palynomorph ratio (T/M-ratio) was calculated by dividing terrestrial palynomorphs (pollen and spores) by aquatic palynomorphs (dinocysts and acritarchs). In general T/M-values are elevated in the organic-rich intervals (Fig. 3h), while minima in the T/M-ratio correspond to organic-poor intervals.

Age-diagnostic dinocyst species include *Lithosphaeridium siphoniphorum siphoniphorum*, a marker species for the CTB interval in the northwest European reference section at Eastbourne (Pearce et al., 2009). The last occurrence of *L. siphoniphorum siphoniphorum* is at 47.81 mbs (Fig. 3f), confirming a latest Cenomanian age.

Dinocyst assemblages are dominated by multiple species of the Peridiniaceae family, i.e., *Paleohystrichophora infusorioides*, *Subtilisphaera pontis-mariae*, *Eurydinium saxoniense*, *Isabelidinium* spp., and *Ginginodinium* spp.. Members of this family have repeatedly been shown to be derived of low-salinity tolerant dinoflagellates in Late Cretaceous and Paleogene successions and likely represent heterotrophic, euryhaline dinoflagellates (e.g. Harland, 1973; Sluijs and Brinkhuis, 2009; Powell et al., 1990; Lewis et al., 1990; Fig. 3c). Other quantitatively important taxa include *Spiniferites* spp. (Fig. 3d) and *Impagidinium* spp. (Fig. 3e), which are generally associated with outer shelf to oceanic environments (e.g. Wall et al., 1977; Harland, 1983; Brinkhuis, 1994). Commonly present are representatives of *Odontochitina*, *Oligosphaeridium*, *Exochosphaeridium*, *Downiesphaeridium*, *Cyclonephelium*, *Lithosphaeridium*, *Achomosphaera*, and *Florentinia* spp., which are, like most encountered pollen and spores, typical for Late Cretaceous dinocyst shelf to bathyal assemblages (e.g. Dodsworth, 2004; Pearce et al., 2009; Peyrot et al., 2012).

4 Discussion

4.1 SST reconstruction

4.1.1 Input of terrestrially derived GDGTs and post-depositional oxidation

Small quantities of iGDGTs as used for determination of TEX_{86} values, are also produced in soils. High input of soil-derived iGDGTs, reflected by elevated BIT index values, might therefore bias TEX_{86}-derived SST reconstructions (Weijers et al., 2006). TEX_{86} and BIT index values for the OAE2-record of the Wunstorf core exhibit a negative linear relation (R^2-value of 0.43; Fig. 4), which may be the result of relatively high input of soil-derived iGDGTs, potentially affecting TEX_{86} values. Previous work has recommended a cut-off value of the BIT index to exclude this effect from TEX_{86}-based paleotemperature reconstructions (Weijers et al., 2006).

Low-TOC sediments have high BIT index values and low TOC-normalized concentrations for brGDGTs and, to a larger extent, iGDGTs (Fig. 5). This is similar to results from TOC-rich turbidites that are affected by post-depositional oxidation (e.g. Huguet et al., 2008; Lengger et al., 2013). This was explained by preferential preservation of soil-derived brGDGTs over marine-derived iGDGTs upon post-depositional oxidation of the turbidites. For the Wunstorf section, the marls and limestones represent depositional phases during which the water column and pore waters of surface sediments contained relatively high concentrations of oxygen, as is evident from bioturbation, low TOC content (Fig. 2b), and low levels of redox-sensitive trace elements (Hetzel et al., 2011). Diagenetic effects caused by the oxidation of biomarkers in the water column and pore waters most likely played a substantial role in this depositional setting. Preferential preservation of brGDGTs is therefore likely responsible for the observed pattern in the BIT-index. Although Lengger et al. (2013) did not find a bias in TEX_{86} values for sediments that suffered post-depositional oxidation, other studies have shown that there can be a considerable post-depositional oxidation effect on TEX_{86} values and thus the paleo-SST reconstructions derived from it (e.g. Huguet et al., 2009). The lin-

ear correlation between TEX_{86} and BIT-index values for the analyzed sediments of the Wunstorf core, is in line with the latter.

Based on the relation between TOC and the BIT-index (Fig. 5a) and the concentrations of the sum of the brGDGTs and crenarcheol (Fig. 5b), we decided to remove reconstructed paleo-SST data with a BIT-index > 0.15. This changes the linear correlation between TEX_{86} and BIT-index, suggesting that samples with a BIT-index > 0.15 are affected by post-depositional oxidation. This results in a dataset in which samples with a BIT-index value between 0.02 and 0.12 are considered for paleo-SST reconstructions, removing the impact of soil derived iGDGTs on the paleo-SST reconstructions.

4.1.2 Trends and absolute values

Trends and values of the reconstructed SSTs at Wunstorf using the TEX_{86}^{H}-calibration of Kim et al. (2010; Fig. 6c) are similar to previous TEX_{86}-based SST reconstructions for OAE2. Previously studied sites were located in the equatorial Atlantic (DSDP Site 367 and ODP Site 1260; Forster et al., 2007) and the mid-latitudes (ODP Site 1276 – Sinninghe Damsté et al., 2010; Bass River – van Helmond et al., 2014; Fig. 1). Potentially due to a lack of reliable TEX_{86} values at the onset of the OAE2-interval (Fig. 6b) the Wunstorf SST record does not capture the rapid warming in SST at the onset of OAE2, previously attributed to a rise in atmospheric CO_2 released by extensive volcanism (e.g. Forster et al., 2007). The Wunstorf SST-record does show, however, a $\sim 5\,°C$ cooling pulse during the early stages of OAE2 (Fig. 6c). Based on its stratigraphic position within the carbon isotope excursion, we attribute this pulse to the Plenus Cold Event (Gale and Christensen, 1996). The Plenus Cold Event, previously recognized as an incursion of boreal fauna in the shelf seas of NW Europe (e.g. Jefferies, 1962; Gale and Christensen, 1996; Voigt et al., 2004), has by now been identified as a substantial cooling event in TEX_{86}-based paleo-SST records at DSDP Site 367, ODP Site 1260, ODP Site 1276, Bass River (all proto-North Atlantic basin; Forster et al., 2007; Sinninghe Damsté et al., 2010; van Helmond et al., 2014) and Wunstorf, suggesting that it was a hemisphere-wide and perhaps even a global signal. This supports the hypothe-

sis that enhanced global carbon burial temporary suppressed atmospheric CO_2 levels during OAE2 (Sinninghe Damsté et al., 2010).

Interestingly, this interval marks the occurrence of the *Cyclonephelium compactum-membraniphorum* complex (*C. comp.-memb.* cplx.) within the OAE2 interval in the

5 Wunstorf core (Fig. 6c and d). This is in accordance with previous records from the Bass River section (van Helmond et al., 2014). Although the biogeographic distribution of this complex is still partly unclear, this suggests that the introduction of *C. comp.-memb.* cplx. at mid-latitude sites in both northwest Europe and the east coast of North-America was quasi-instantaneous and linked to the Plenus Cold Event

10 No significant difference in the reconstructed SSTs is recorded between the black shales and the more TOC-lean marls and limestones. This suggests that the cyclic deposition of black shales during OAE2 in the LSB was not primarily driven by changes in SST.

Average SSTs for the OAE2-interval at Wunstorf are higher than at Bass River (New

15 Jersey Shelf), DSDP Site 367 (Cape Verde Basin), ODP Site 1260 (Demarara Rise), and Site 1276 (North Atlantic; Table 1), which may perhaps be an artefact of the low resolution achieved for the Plenus Cold Event at Wunstorf. Reconstructions of absolute temperatures based on TEX86 at values significantly exceeding the modern calibration may yield significant errors. Nonetheless, the warm and relatively stable background

20 SSTs for Wunstorf ($\sim$ 37 °C) suggest that SSTs on the European shelf were exceptionally high and supports the notion that thermal gradients were substantially reduced during the Late Cretaceous greenhouse world (e.g. Baron, 1983; Huber et al., 1995).

4.2 Hydrology

Although pollen rank among the most resistant groups of palynomorphs (Traverse,

25 1994), there is evidence that pollen grains are degraded relatively rapidly (< 10 kyr) in the presence of diffusively introduced oxygen (e.g. Keil et al., 1994). This may perhaps explain why absolute pollen and spores concentrations are higher in the black shales, deposited under anoxic conditions. This contrasts with the organic lean marls

and limestones deposited in phases in which pore waters of surface sediments contained relatively high concentrations of oxygen. Despite evidence for some preferential preservation of some groups of dinocysts in Quaternary sediments (e.g. Zonneveld et al., 1997; Versteegh and Zonneveld, 2002), in general the same holds for dinocysts,
5 explaining higher dinocyst concentrations in the black shales. Thin-walled dinocysts, e.g. *Paleohystrichophora infusorioides*, which would be expected to be lost from sediments upon oxidation most rapidly, are, however, commonly present in the organic lean marls and limestones. This shows that the preferential preservation of palynomorphs, and dinocysts in particular, may not be so straightforward in older sediments, e.g. the
10 Cretaceous, as previously reported for some Quaternary sediments (e.g. Zonneveld et al., 1997; Versteegh and Zonneveld, 2002).

Pollen and spores are transported to the marine environment by a wide range of processes ranging from river discharge, wind, to birds and insects (e.g. Traverse and Ginsburg, 1966; Thomson, 1986; Feinsinger and Busby, 1987). Particularly saccate
15 gymnosperm pollen (bisaccates) may be transported by eolian pathways (e.g. Heusser, 1988). Palynological assemblages at Wunstorf contain relatively low amounts of saccate gymnosperm pollen (Fig. 6e; Prauss, 2006), suggesting that most pollen and spores encountered at Wunstorf were transported to the ocean by fluvial processes. The relatively high amounts of pollen and spores in the black shales at Wunstorf are
20 therefore interpreted to represent phases of enhanced run-off. Enhanced run-off most likely resulted from increased (seasonal) precipitation over north and mid-European landmasses, assuming that these yielded significant vegetation cover. Regarding the distance to the coring site, non-saccate pollen and spores most likely originated from the Rheno-Bohemian Massif, which is in accordance with the prevailing paleo-wind
25 directions (Hay and Floegel, 2012). Enhanced (seasonal) influx of fresh, low-density, surface waters could well have stratified the water column, leading to low-oxygen levels in bottom waters. This is also indicated by high abundances of bacterivorous ciliates (Blumenberg and Wiese, 2012), which graze on the interfaces of stratified water bodies (Sinninghe Damsté et al., 1995), supporting the presence of a chemocline in the water

column. A persistent stratification of the water column ultimately leads to bottom water anoxia and the formation of black shales. The coupling of the rhythmical occurrence of the black shale layers to the precession cycle (Voigt et al., 2008) suggests that changes in the hydrological cycle were controlled by Earth's orbital parameters.

4.3 Marine productivity

High abundances of dinocysts and organic matter in general may result from both enhanced marine primary productivity and an improved preservation potential for organic matter during black shale deposition. In modern oceans, most peridinioid dinocysts are produced by heterotrophic dinoflagellates, whilst most gonyaulacoid dinocysts are derived from autotrophic taxa (Lewis et al., 1990). As a consequence, the ratio between peridinioids and gonyaulacoids (P/G-ratio) has been employed widely as a proxy for paleoproductivity (Sluijs et al., 2005). In the Wunstorf OAE2-section, the P/G-ratio reaches maximum values within the different black shale couplets, implying that productivity was elevated during their deposition (Fig. 6f). Furthermore the peridinioids encountered at Wunstorf belong to the Peridiniaceae family, which has been shown to be low-salinity tolerant (e.g. Harland, 1973; Sluijs and Brinkhuis, 2009). Together, this suggests that during seasons of high precipitation and run-off that introduced nutrients a low-salinity, high-productivity surface layer existed in the Lower Saxony Basin. This hypothesis is supported by assemblages of calcareous nannofossils, showing a shift from a generally oligotrophic ecosystem to more mesotrophic or even eutrophic conditions during black shale deposition (Linnert et al., 2010).

Enhanced marine primary productivity likely contributed to the establishment of bottom water anoxia by increasing the flux of organic matter to the seafloor, depleting bottom water oxygen concentrations upon decay.

5   Conclusions

Despite differences in the preservation of organic matter throughout the OAE2 interval at Wunstorf, the general trend in reconstructed SSTs, including the cooling phase associated with the Plenus Cold Event, is consistent with the results of previous studies that targeted the proto-North Atlantic. Hence, the SST trend recorded at Wunstorf and the other sites was of at least hemispheric significance. Reconstructed SSTs do not substantially differ between black shales and less organic-rich deposits, implying that temperature was not the critical factor for the cyclic deposition of organic matter. Absolute SSTs for the Wunstorf OAE2 section show little or no difference in comparison with SST reconstructions for sites located at lower latitudes, which were evaluated using the same proxy and the same methodology. This confirms that thermal gradients were much reduced during the Late Cretaceous (Barron, 1983; Huber et al., 1995).

The dinocyst complex *Cyclonephelium compactum–C. membraniphorum*, previously linked to the Plenus Cold Event (van Helmond et al., 2014), was encountered at the respective level at Wunstorf, suggesting that its occurrence is indeed linked to this cooling. Its continued presence in the remainder of the record suggests, however, that other paleoenviromental factors were also critical in controlling its distribution.

Black shale deposition for the OAE2 interval at Wunstorf relied on precession-driven changes (Voigt et al., 2008). We conclude, based on relatively high numbers of terrestrially derived pollen and spores and freshwater tolerating dinocysts in the black shale intervals, that precession drove variations in the hydrological cycle. This caused (seasonal) freshwater stratification of the water column and likely enhanced primary production, ultimately culminating in bottom water anoxia and black shale formation. An orbitally controlled hydrological cycle may have been a critical factor triggering mechanism for other cyclic OAE2 sites located in the proto-Atlantic and Western Interior Seaway at similar latitudes as well.

The Supplement related to this article is available online at doi:10.5194/cpd-10-3755-2014-supplement.

References

Arthur, M. A., Dean, W. E., and Pratt, L. M.: Geochemical and climatic effects of increased marine organic carbon burial at the Cenomanian/Turonian boundary, Nature, 335, 714–717, doi:10.1038/335714a0, 1988.

Barclay, R. S., McElwain, J. C., and Sageman, B. B.: Carbon sequestration activated by a volcanic CO_2 pulse during Oceanic Anoxic Event 2, Nat. Geosci., 3, 205–208, doi:10.1038/NGEO757, 2010.

Barron, E. J.: A warm, equable Cretaceous: the nature of the problem, Earth-Sci. Rev., 19, 305–338, doi:10.1016/0012-8252(83)90001-6, 1983.

Blättler, C. L., Jenkyns, H. C., Reynard, L. M., and Henderson, G. M.: Significant increases in global weathering during Oceanic Anoxic Events 1a and 2 indicated by calcium isotopes, Earth Planet. Sc. Lett., 309, 77–88, doi:10.1016/j.epsl.2011.06.029, 2011.

Blumenberg, M. and Wiese, F.: Imbalanced nutrients as triggers for black shale formation in a shallow shelf setting during the OAE 2 (Wunstorf, Germany), Biogeosciences, 9, 4139–4153, doi:10.5194/bg-9-4139-2012, 2012.

Title Page

Abstract | Introduction

Conclusions | References

Tables | Figures

|◄ | ►|

◄ | ►

Back | Close

Full Screen / Esc

Printer-friendly Version

Interactive Discussion

Bice, K. L., Birgel, D., Meyers, P. A., Dahl, K. A., Hinrichs, K.-U., and Norris, R. D.: A multiple proxy and model study of the Cretaceous upper ocean temperatures and atmospheric CO_2 concentrations, Paleoceanography, 21, PA2002, doi:10.1029/2005PA001203, 2006.

Brinkhuis, H.: Late Eocene to Early Oligocene dinoflagellate cysts from the Priabonian type-area (northeast Italy): biostratigraphy and palaeoenvironmental interpretation. Palaeogeogr. Palaeocl., 107, 121–163, doi:10.1016/0031-0182(94)90168-6, 1994.

Creaney, S. and Passey, Q. R.: Recurring Patterns of Total Organic Carbon and Source Rock Quality within a Sequence Stratigraphic Framework, AAPG Bull., 77, 386–401, 1993.

Dodsworth, P.: The palynology of the Cenomanian–Turonian (Cretaceous) boundary succession at Aksudere in Crimea, Ukraine, Palynology, 28, 129–141, doi:10.2113/28.1.129, 2004.

Du Vivier, A. D. C., Selby, D., Sageman, B. B., Jarvis, I., Gröcke, D. R., and Voigt, S.: Marine $^{187}Os/^{188}Os$ isotope stratigraphy reveals the interaction of volcanism and ocean circulation during Oceanic Anoxic Event 2, Earth Planet. Sc. Lett., 389, 23–33, doi:10.1016/j.epsl.2013.12.024, 2014.

Erbacher, J., Thurow, J., and Littke, R.: Evolution patterns of radiolariaand organic matter variations: a new approach to identify sea-level changes in mid-Cretaceous pelagic environments, Geology, 6, 499–502, doi:10.1130/0091-7613(1996)024<0499:EPORAO>2.3.CO;2, 1996.

Erbacher, J., Mutterlose, J., Wilmsen, M., Wonik, T., and Party, W. D. S.: The Wunstorf Drilling Projetc: coring a global stratigraphic reference section of the Oceanic Anoxic Event 2, Sci. Drill., 4, 19–21, 2007.

Ernst, G., Wood, C. J., and Hilbrecht, H.: The Cenomanian-Turonian boundary problem in NW-Germany with comments on the north-south correlation to the Regensburg area, Bull. Geol. Soc. Den., 33, 103–113, 1984.

Feinsinger, P. and Busby, W. H.: Pollen carryover: experimental comparisons between morphs of Palicourea lasiorrhachis (Rubiaceae), a distylous, bird-pollinated, tropical treelet, Oecologia, 73, 231–235, 1987.

Fensome, R. A. and Williams, G. L.: The Lentin and Williams Index of Fossil Dinoflagellates, 2004 Edition, American Association of Stratigraphic Palynologists Contribution Series 42, 909 pp., 2004.

Forster, A., Schouten, S., Moriya, K., Wilson, P. A., and Sinninghe Damsté, J. S.: Tropical warming and intermittent cooling during the Cenomanian/Turonian Oceanic Anoxic Event (OAE 2): sea surface temperature records from the equatorial Atlantic, Paleoceanography, 22, PA1219, doi:10.1029/2006PA001349, 2007.

Freshwater forced black shale deposition during OAE2

N. A. G. M. van Helmond et al.

Title Page

Abstract | Introduction

Conclusions | References

Tables | Figures

|◄ | ►|

◄ | ►

Back | Close

Full Screen / Esc

Printer-friendly Version

Interactive Discussion

Forster, A., Kuypers, M. M. M., Turgeon, S. C., Brumsack, H.-J., Petrizzo, M. R., Sinninghe Damsté, J. S.: The Cenomanian/Turonian oceanic anoxic event in the South Atlantic: new insights from a geochemical study of DSDP Site 530A, Palaeogeogr. Palaeocl., 267, 256–283, doi:10.1016/j.palaeo.2008.07.006, 2008.

5 Gale, A. S. and Christensen, W. K.: Occurrence of the belemnite Actinocamax plenus in the Cenomanian of SE France and its significance, Bull. Geol. Soc. Den., 43, 68–77, 1996.

Hancock, J. M. and Kauffman, E. G.: The great transgressions of the Late Cretaceous. J. Geol. Soc. London, 136, 175–186, 1979.

Harland, R.: Dinoflagellate cysts and acritarchs from the Bearpaw Formation (Upper Campa-
10 nian) of southern Alberta, Canada, Palaeontology, 16, 665–706, 1973.

Harland, R.: Distribution maps of recent dinoflagellate cysts in bottom sediments from the North Atlantic Ocean and adjacent seas, Palaeontology, 26, 321–387, 1983.

Hay, W. W. and Flögel, S.: New thoughts about the Cretaceous climate and oceans, Earth-Sci. Rev., 115, 262–272, doi:10.1016/j.earscirev.2012.09.008, 2012.

15 Hetzel, A., März, C., Vogt, C., and Brumsack, H.-J.: Geochemical environment of Cenomanian–Turonian black shale deposition at Wunstorf (northern Germany), Cretaceous Res., 32, 480–494, doi:10.1016/j.cretres.2011.03.004, 2011.

Heusser, L. E.: Pollen distribution in marine sediments on the continental margin off northern California, Mar. Geol., 80, 131–147, 1988.

20 Hopmans, E. C., Weijers, J. W. H., Schefuß, E., Herfort, L., Sinninghe Damsté, J. S., and Schouten, S.: A novel proxy for terrestrial organic matter in sediments based on branched and isoprenoid tetraether lipids, Earth Planet. Sc. Lett., 224, 107–116, doi:10.1016/j.epsl.2004.05.012, 2004.

Huber, B. T., Hodell, D. A., and Hamilton, C. P.: Middle–Late Cretaceous climate
25 of the southern high latitudes: stable isotopic evidence for minimal equator-to-pole thermal gradients, Geol. Soc. Am. Bull., 107, 1164–1191, doi:10.1130/0016-7606(1995)107<1164:MLCCOT>2.3.CO;2, 1995.

Huguet, C., Hopmans, E. C., Febo-Ayala, W., Thompson, D. H., Sinninghe Damsté, J. S., and Schouten, S.: An improved method to determine the absolute abundance
30 of glycerol dibiphytanyl glycerol tetraether lipids, Org. Geochem., 37, 1036–1041, doi:10.1016/j.orggeochem.2006.05.008, 2006.

Freshwater forced black shale deposition during OAE2

N. A. G. M. van Helmond et al.

Title Page

Abstract	Introduction
Conclusions	References
Tables	Figures

|◄   ►|

◄   ►

Back   Close

Full Screen / Esc

Printer-friendly Version

Interactive Discussion

Huguet, C., de Lange, G. J., Middelburg, J. J., Sinninghe Damsté, J. S., and Schouten, S.: Selective preservation of soil organic matter in oxidized marine sediments (Madeira Abyssal Plain), Geochim. Cosmochim. Ac., 72, 6061–6068, doi:10.1016/j.gca.2008.09.021, 2008.

Huguet, C., Kim, J.-H., de Lange, G. J., Sinninghe Damsté, J. S., and Schouten, S.: Effects of long-term oxic degradation on the $U_{37}^{K'}$, TEX$_{86}$ and BIT organic proxies, Org. Geochem., 40, 1188–1194, doi:10.1016/j.orggeochem.2009.09.003, 2009.

Jefferies, R. P. S.:The palaeoecology of the Actinocamax plenus subzone (lowest Turonian) in the Anglo-Paris Basin, Palaeontology, 4, 609–647, 1962.

Jenkyns, H. C.: Geochemistry of oceanic anoxic events, Geochem. Geophy. Geosy., 11, Q03004, doi:10.1029/2009GC002788, 2010.

Junium, C. K. and Arthur, M. A.: Nitrogen cycling during the Cretaceous, Cenomanian-Turonian Oceanic Anoxic Event II, Geochem. Geophy. Geosy., 8, Q03002, doi:10.1029/2006GC001328, 2007.

Keil, R. G., Hu, E. S., Tsamakis, E. C., and Hedges, J. I.: Pollen in marine sediments as an indicator of oxidation of organic matter, Nature, 369, 639–641, doi:10.1038/369639a0, 1994.

Kerr, A. C.: Oceanic plateau formation: a cause of mass extinction and black shale deposition around the Cenomanian–Turonian boundary?, J. Geol. Soc. London, 155, 619–626, doi:10.1144/gsjgs.155.4.0619, 1998.

Kim, J.-H., van der Meer, J., Schouten, S., Helmke, P., Willmott, V., Sangiorgi, F., Koç, N., Hopmans, E. C., and Sinninghe Damsté, J. S.: New indices and calibrations derived from the distribution of crenarchaeal isoprenoid tetraether lipids: implications for past sea surface temperature reconstructions, Geochim. Cosmochim. Ac., 74, 4639–4654, doi:10.1016/j.gca.2010.05.027, 2010.

Kuroda, J., Ogawa, N., Tanimizu, M., Coffin, M., Tokuyama, H., Kitazato, H., and Ohkouchi, N.: Contemporaneous massive subaerial volcanism and late cretaceous Oceanic Anoxic Event 2, Earth Planet. Sc. Lett., 256, 211–223, doi:10.1016/j.epsl.2007.01.027, 2007.

Kuypers, M. M. M., Lourens, L. J., Rijpstra, W. I. C., Pancost, R. D., Nijenhuis, I. A., and Sinninghe Damsté, J. S.: Orbital forcing of organic carbon burial in the proto-North Atlantic during oceanic anoxic event 2, Earth Planet. Sc. Lett., 228, 465–482, doi:10.1016/j.epsl.2004.09.037, 2004a.

Kuypers, M. M. M., van Breugel, Y., Schouten, S., Erba, E., and Sinninghe Damsté, J. S.: N$_2$-fixing cyanobacteria supplied nutrient N for Cretaceous oceanic anoxic events, Geology, 32, 853–856, doi:10.1130/G20458.1, 2004b.

Freshwater forced black shale deposition during OAE2

N. A. G. M. van Helmond et al.

Title Page

Abstract | Introduction

Conclusions | References

Tables | Figures

|◄ | ►|

◄ | ►

Back | Close

Full Screen / Esc

Printer-friendly Version

Interactive Discussion

Lengger, S. K., Kraaij, M., Tjallingii, R., Baas, M., Stuut, J. B., Hopmans, E. C., Sinninghe Damsté, J. S., and Schouten, S.: Differential degradation of intact polar and core glycerol dialkyl glycerol tetraether lipids upon post-depositional oxidation, Org. Geochem., 65, 83–93, doi:10.1016/j.orggeochem.2013.10.004, 2013.

Lewis, J., Dodge, J. D., and Powell, J.: Quaternary dinoflagllate cysts from the upwelling system offshore Peru, Hole 686B, ODP Leg 112, in: Proceedings of the Ocean Drilling Program, Scientific Results, edited by: Suess, E., von Huene, R., Emeis, K.-C., Bourgois, J., del C. Cruzado Castaheda, J., De Wever, P., Eglinton, G., Garrison, R., Greenberg, M., Herrera Paz, E., Hill, P., Ibaraki, M., Kastner, M., Kemp, A. E. S., Kvenvolden, K., Langridge, R., Lindsley-Griffin, N., Marsters, J., Martini, E., McCabe, R., Ocola, L., Resig, J., Wilfredo Sanchez Fernandez, A., Schrader, H. J., Thornburg, T., Wefer, G., and Yamano, M., 112, 323–328, 1990.

Linnert, C., Mutterlose, J., and Erbacher, J.: Calcareous nannofossils of the Cenomanian/Turonian boundary interval from the Boreal Realm (Wunstorf, northwest Germany), Mar. Micropaleontol., 74, 38–58, doi:10.1016/j.marmicro.2009.12.002, 2010.

Marshall, K. L. and Batten, D. J.: Dinoflagellate cyst associations in Cenomanian–Turonian "black shale" sequences of northern Europe, Rev. Palaeobot. Palyno., 54, 85–103, 1988.

Meyers, S. R., Sageman, B. B., and Arthur, M. A.: Obliquity forcing and the amplification of high-latitude climate processes during Oceanic Anoxic Event 2, Paleoceanography, 27, PA3212, doi:10.1029/2012PA002286, 2012.

Miller, K. G., Kominz, M. A., Browning, J. V., Wright, J. D., Mountain, G. S., Katz, M. E., Sugarman, P. J., Carter, B. S., Christie-Blick, N., and Pekar, S. F.: The Phanerozoic record of global sea-level change, Science, 310, 1293–1298, doi:10.1126/science.1116412, 2005.

Mort, H. P., Adatte, T., Föllmi, K. B., Keller, G., Steinmann, P., Matera, V., Berner, Z., Stuben, D.: Phosphorus and the roles of productivity and nutrient recycling during oceanic anoxic event 2, Geology, 35, 483–486, doi:10.1130/G23475A.1, 2007.

Pearce, M. A., Jarvis, I., and Tocher, B. A.: The Cenomanian-Turonian boundary event, OAE 2 and palaeoenvironmental change in epicontinental seas: new insights from the dinocyst and geochemical records, Palaeogeograph. Palaeocl., 280, 207–234, doi:10.1016/j.palaeo.2009.06.012, 2009.

Peyrot, D., Barroso-Barcenilla, F., and Feist-Burkhardt, S.: Palaeoenvironmental controls on late Cenomanian–early Turonian dinoflagellate cyst assemblages from Condemios (Central Spain), Rev. Palaeobot. Palyno., 180, 25–40, doi:10.1016/j.revpalbo.2012.04.008, 2012.

Title Page

Abstract | Introduction

Conclusions | References

Tables | Figures

◀ | ▶

◀ | ▶

Back | Close

Full Screen / Esc

Printer-friendly Version

Interactive Discussion

Pogge von Strandmann, P. A. E., Jenkyns, H. C., and Woodfine, R. G.: Lithium isotope evidence for enhanced weathering during Oceanic Anoxic Event 2, Nat. Geosci., 6, 668–672, doi:10.1038/ngeo1875, 2013.

Poulsen, J. C., Barron, E. J., Arthur, A., and Peterson, H.: Response of the mid-Cretaceous global oceanic circulation to tectonic and CO_2 forcings, Paleoceanography, 16, 576–592, doi:10.1029/2000PA000579, 2001.

Powell, A. J., Dodge, J. D., and Lewis, J.: Late Neogene to Pleistocene palynological facies of the Peruvian continental margin upwelling, Leg 112, in: Proceedings of the Ocean Drilling Program, Scientific Results, edited by: Suess, E., von Huene, R., Emeis, K.-C., Bourgois, J., del C. Cruzado Castaheda, J., De Wever, P., Eglinton, G., Garrison, R., Greenberg, M., Herrera Paz, E., Hill, P., Ibaraki, M., Kastner, M., Kemp, A. E. S., Kvenvolden, K., Langridge, R., Lindsley-Griffin, N., Marsters, J., Martini, E., McCabe, R., Ocola, L., Resig, J., Wilfredo Sanchez Fernandez, A., Schrader, H. J., Thornburg, T., Wefer, G., and Yamano, M., 112, 297–321, 1990.

Prauss, M. L.: The Cenomanian–Turonian Boundary Event (CTBE) at Wunstorf, northwest Germany, as reflected by marine palynology, Cretaceous Res., 27, 872–886, doi:10.1016/j.cretres.2006.04.004, 2006.

Schlanger, S. O. and Jenkyns, H. C.: Cretaceous oceanic anoxic events: causes and consequences, Geol. Mijnbouw, 55, 179–184, 1976.

Schouten, S., Hopmans, E. C., Schefuss, E., and Sinninghe Damsté, J. S.: Distributional variations in marine crenarchaeotal Membrane lipids: a new tool for reconstructing ancient sea water temperatures?, Earth Planet. Sci. Lett., 204, 265–274, doi:10.1016/S0012-821X(02)00979-2, 2002.

Schouten, S., Hopmans, E. C., Forster, A., van Breugel, Y., Kuypers, M. M. M., and Sinninghe Damsté, J. S.: Extremely high sea-surface temperatures at low latitudes during the middle Cretaceous as revealed by archaeal membrane lipids, Geology, 31, 1069–1072, doi:10.1130/G19876.1, 2003.

Schouten, S., Hopmans, E. C., and Sinninghe Damsté, J. S.: The effect of maturity and depositional redox conditions on archaeal tetraether lipid palaeothermometry, Org. Geochem., 35, 567–571, doi:10.1016/j.orggeochem.2004.01.012, 2004.

Schouten, S., Huguet, C., Hopmans, E. C., Kienhuis, M. V. M., and Sinninghe Damsté: J. S.: Improved analytical methodology for TEX_{86} paleothermometry by high performance liquid

Freshwater forced black shale deposition during OAE2

N. A. G. M. van Helmond et al.

Title Page

Abstract | Introduction

Conclusions | References

Tables | Figures

◄◄ | ►►

◄ | ►

Back | Close

Full Screen / Esc

Printer-friendly Version

Interactive Discussion

chromatography/atmospheric pressure chemical ionization-mass spectrometry, Anal. Chem., 79, 2940–2944, doi:10.1021/ac062339v, 2007.

Sinninghe Damsté, J. S., Kenig, F., Koopmans, M. P., Köster, J., Schouten, S., Hayes, J. M., and de Leeuw, J.: Evidence for gammacerane as an indicator of water column stratification, Geochim. Cosmochim. Ac., 59, 1895–1900, doi:10.1016/0016-7037(95)00073-9, 1995.

Sinninghe Damsté, J. S., Kuypers, M. M. M., Pancost, R. D., and Schouten, S.: The carbon isotopic response of algae, (cyano)bacteria, archaea and higher plants to the late Cenomanian perturbation of the global carbon cycle: insights from biomarkers in black shales from the Cape Verde Basin (DSDP Site 367), Org. Geochem., 39, 1703–1718, doi:10.1016/j.orggeochem.2008.01.012, 2008.

Sinninghe Damsté, J. S., van Bentum, E. C., Reichart, G.-J., Pross, J., and Schouten, S.: A CO_2 decrease-driven cooling and increased latitudinal temperature gradient during the mid-Cretaceous Oceanic Anoxic Event 2, Earth Planet. Sc. Lett., 293, 97–103, doi:10.1016/j.epsl.2010.02.027, 2010.

Sluijs, A. and Brinkhuis, H.: A dynamic climate and ecosystem state during the Paleocene-Eocene Thermal Maximum: inferences from dinoflagellate cyst assemblages on the New Jersey Shelf, Biogeosciences, 6, 1755–1781, doi:10.5194/bg-6-1755-2009, 2009.

Sluijs, A., Pross, J., and Brinkhuis, H.: From greenhouse to icehouse; organic-walled dinoflagellate cysts as paleoenvironmental indicators in the Paleogene, Earth-Sci. Rev., 68, 281–315, doi:10.1016/j.earscirev.2004.06.001, 2005.

Snow, L. J., Duncan, R. A., and Bralower, T. J.: Trace element abundances in the Rock Canyon anticline, Pueblo, Colorado, marine sedimentary section and their relationship to Caribbean plateau construction and oxygen anoxic event 2, Paleoceanography, 20, PA3005, doi:10.1029/2004PA001093, 2005.

Thomson, J. D.: Pollen transport and deposition by bumble bees in Erythronium: influences of floral nectar and bee grooming, J. Ecol., 74, 329–341, 1986.

Traverse, A.: Sedimentation of Organic Particles, Cambridge University Press, New York, 544 pp., 1994.

Traverse, A. and Ginsburg, R. N.: Palynology of the surface sediments of Great Bahama Bank, as related to water movement and sedimentation, Mar. Geol., 4, 417–459, 1966.

Tsikos, H., Jenkyns, H. C., Walsworth-Bell, B., Petrizzo, M. R., Forster, A., Kolonic, S., Erba, E., Premoli Silva, I., Baas, M., Wagner, T., and Sinninghe Damsté, J. S.: Carbon-isotope stratigraphy recorded by the Cenomanian–Turonian Oceanic Anoxic Event: correlation and implica-

Freshwater forced black shale deposition during OAE2

N. A. G. M. van Helmond et al.

Title Page

Abstract	Introduction
Conclusions	References
Tables	Figures

|◀| |▶|

|◀| |▶|

Back | Close

Full Screen / Esc

Printer-friendly Version

Interactive Discussion

tions based on three key localities, J. Geol. Soc. London, 161, 711–719, doi:10.1144/0016-764903-077, 2004.

Turgeon, S. C., Creaser, R. A.: Cretaceous oceanic anoxic event 2 triggered by a massive magmatic episode, Nature, 454, 323–326, doi:10.1038/nature07076, 2008.

Van Helmond, N. A. G. M., Sluijs, A., Reichart, G. J., Sinninghe Damsté, J. S., Slomp, C. P., and Brinkhuis, H.: A perturbed hydrological cycle during Oceanic Anoxic Event 2, Geology, 42, 123–126, doi:10.1130/G34929.1, 2014.

Versteegh, G. J. M. and Zonneveld, K. A. F.: Use of selective degradation to separate preservation from productivity, Geology, 30, 615–618, doi:10.1130/0091-7613(2002)030<0615:UOSDTS>2.0.CO;2, 2002.

Voigt, S., Gale, A. S., and Flögel, S.: Midlatitude shelf seas in the Cenomanian-Turonian greenhouse world: temperature evolution and North Atlantic circulation, Paleoceanography, 19, PA4020, doi:10.1029/2004PA001015, 2004.

Voigt, S., Gale, A. S., and Voigt, T.: Sea-level change, carbon cycling and palaeoclimate during the Late Cenomanian of northwest Europe; An integrated palaeoenvironmental analysis, Cretaceous Res., 27, 836–858, doi:10.1016/j.cretres.2006.04.005, 2006.

Voigt, S., Erbacher, J., Mutterlose, J., Weiss, W., Westerhold, T., Wiese, F., Wilmsen, M., and Wonik, T.: The Cenomanian–Turonian of the Wunstorf section (north Germany): global stratigraphic reference section and new orbital time scale for oceanic anoxic event 2, Newsl. Stratigr., 43, 65–89, doi:10.1127/0078-0421/2008/0043-0065, 2008.

Wall, D., Dale, B., Lohmann, G. P., and Smith, W. K.: The environment and climatic distribution of dinoflagellate cysts in modern marine sediments from regions in the North and South Atlantic Oceans and adjacent seas, Mar. Micropaleontol, 2, 121–200, 1977.

Weijers, J. W. H., Schouten, S., Spaargaren, O. C., and Sinninghe Damsté, J. S.: Occurrence and distribution of tetraether membrane lipids in soils: implications for the use of the TEX_{86} proxy and the BIT index, Org. Geochem., 37, 1680–1693, doi:10.1016/j.orggeochem.2006.07.018, 2006.

Wilmsen, M.: Sequence stratigraphy and palaeoceanography of the Cenomanian stage in northern Germany, Cretaceous Res., 24, 525–568, doi:10.1016/S0195-6671(03)00069-7, 2003.

Zonneveld, K. A. F., Versteegh, G. J. M., and De Lange, G. J.: Preservation of organic walled dinoflagellate cysts in different oxygen regimes: a 10 000 yr natural experiment, Mar. Micropaleontol., 29, 393–405, doi:10.1016/S0377-8398(96)00032-1, 1997.

Title Page

Abstract | Introduction

Conclusions | References

Tables | Figures

|◄ | ►|

◄ | ►

Back | Close

Full Screen / Esc

Printer-friendly Version

Interactive Discussion

Table 1. Overview of the different sites for which TEX_{86}-paleothermometry was applied over the OAE2-interval, and TEX_{86} values and paleo-SST ranges and averages.

Site	Estimated paleolatitude	TEX_{86} range (average)	Reconstructed paleo-SST[a] range (average)
ODP Site 367[b]	5° N	0.84–0.95 (0.90)	33–37 °C (36 °C)
ODP Site 1260[b]	0°	0.85–0.95 (0.92)	34–37 °C (36 °C)
ODP Site 1276[c]	30° N	0.74–0.96 (0.90)	30–37 °C (36 °C)
Bass River[d]	30° N	0.84–0.95 (0.91)	33–37 °C (36 °C)
Wunstorf	40° N	0.80–0.99 (0.93)	32–38 °C (36 °C)

[a] Based on the TEX_{86}^{H} calibration by Kim et al. (2010),

[b] Forster et al. (2007),

[c] Sinninghe Damsté et al. (2010),

[d] van Helmond et al. (2014).
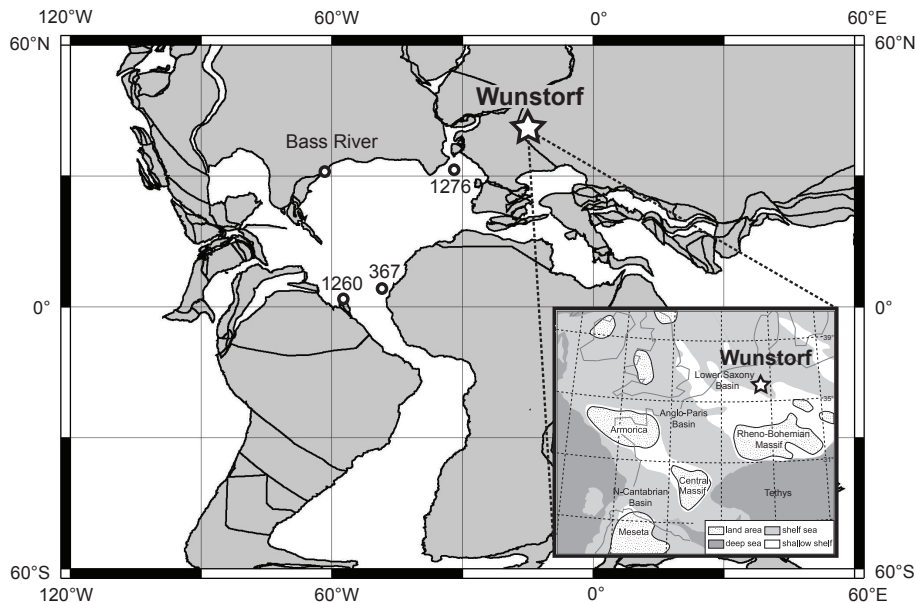
Figure 1. Paleotectonic reconstruction for the Cenomanian/Turonian boundary time interval, with the location of the Wunstorf core and sections with previously published TEX$_{86}$-based SST-records: Bass River, DSDP site 367, ODP sites 1260 and 1276 indicated (map generated at http://www.odsn.de/odsn/services/paleomap/paleomap.html). Inset map shows a detailed paleogeographic reconstruction of central and western Europe, including the location of the Wunstorf core (modified from Voigt et al., 2004).
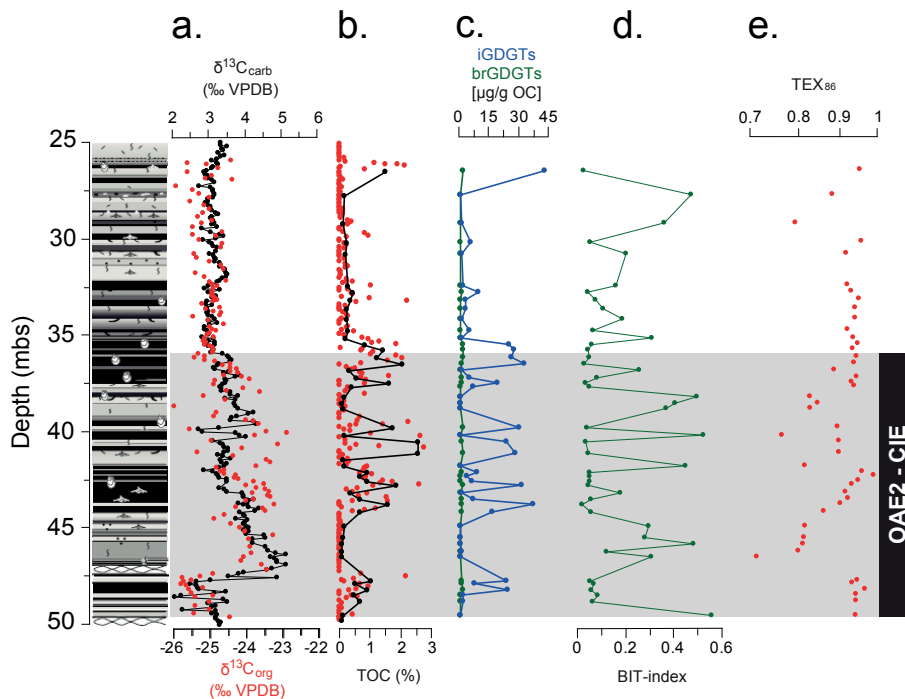
Figure 2. Geochemical results for the Cenomanian–Turonian transition of the Wunstorf core. Stratigraphy from Voigt et al. (2008). **(a)** $\delta^{13}C_{carb}$ (Voigt et al., 2008) and $\delta^{13}C_{org}$ (du Vivier et al., 2014; red). **(b)** Total organic carbon (TOC; black, this study; red, Hetzel et al., 2011). **(c)** concentrations of summed iGDGTs and summed brGDGTs [$\mu g\,g^{-1}$ OC]. **(d)** BIT-index. **(e)** TEX$_{86}$-values. The grey zone indicates the OAE2 interval after Voigt et al. (2008). mbs = meters below surface.
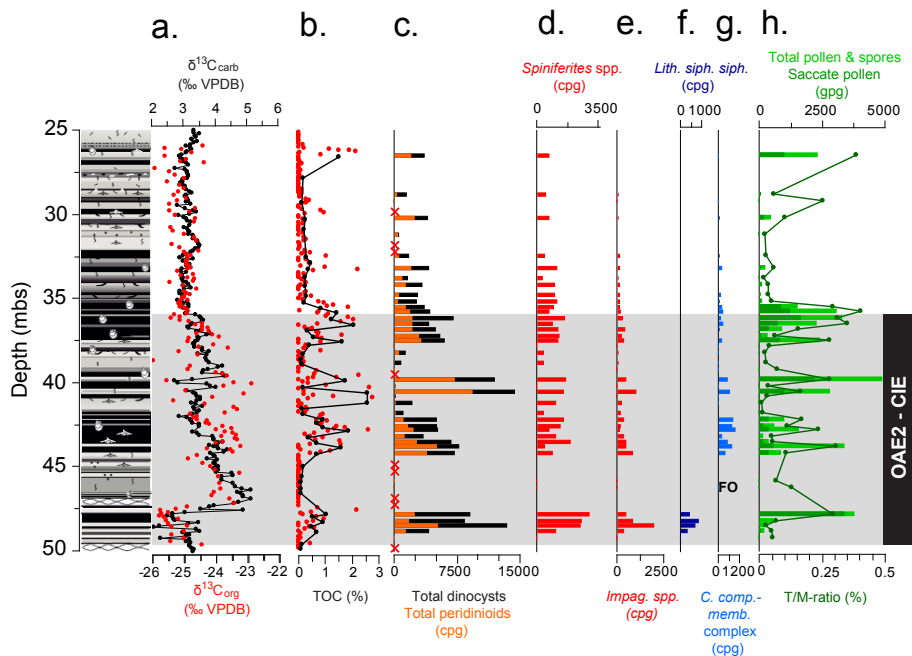
Figure 3. Geochemical and palynological results for the Cenomanian–Turonian transition of the Wunstorf core. Stratigraphy from Voigt et al. (2008). **(a)** $\delta^{13}C_{carb}$ (Voigt et al., 2008) and $\delta^{13}C_{org}$ (du Vivier et al., 2014; red). **(b)** Total organic carbon (TOC; black, this study; red, Hetzel et al., 2011). **(c)** Total dinocyst concentrations (black) and total peridinioidal cysts (orange) per gram sediment dry weight (cpg). **(d)** Dinocyst species *Spiniferites* spp. (cpg). **(e)** Dinocyst species *Impagidinium* spp. (cpg). **(f)** Dinocyst species *Lithosphaeridium siphoniphorum siphoniphorum* (cpg). **(g)** Dinocyst species *Cyclonephelium compactum – C. membraniphorum* complex (cpg). **(h)**. Terrestrial vs. marine palynomorphs (T/M-ratio) and total pollen and spores in grains per dry gram of sediment (gpg), saccate gymnosperm pollen in dark green The grey zone indicates the OAE2 interval after Voigt et al. (2008). mbs = meters below surface.

Title Page

Abstract | Introduction

Conclusions | References

Tables | Figures

|◄ | ►|

◄ | ►

Back | Close

Full Screen / Esc

Printer-friendly Version

Interactive Discussion
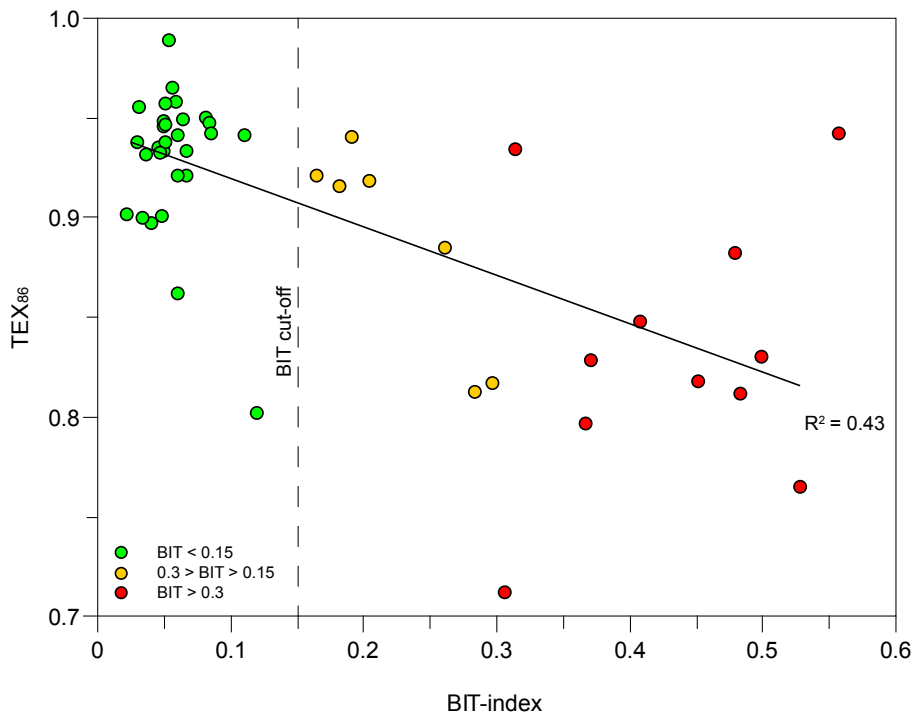
Figure 4. Cross plot of TEX$_{86}$ vs. BIT-index values.
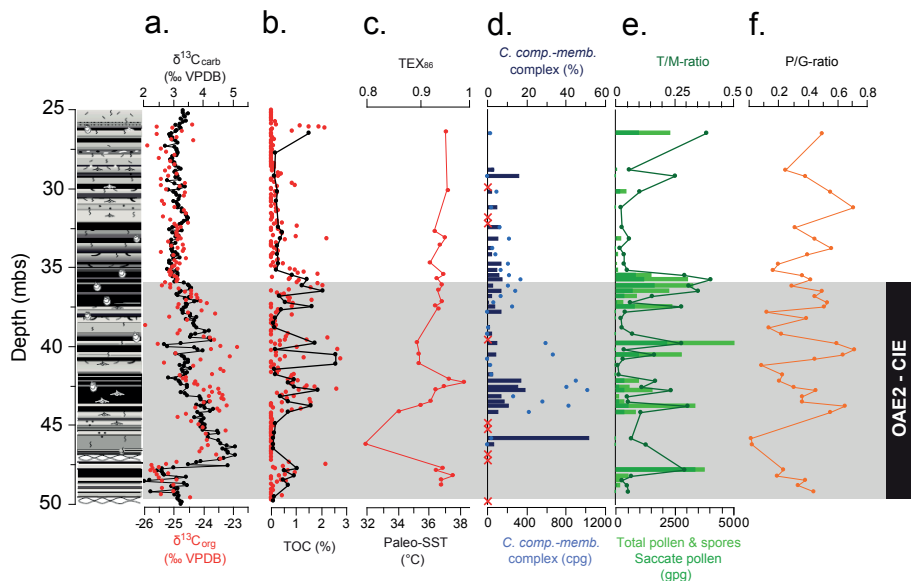
Printer-friendly Version

Interactive Discussion
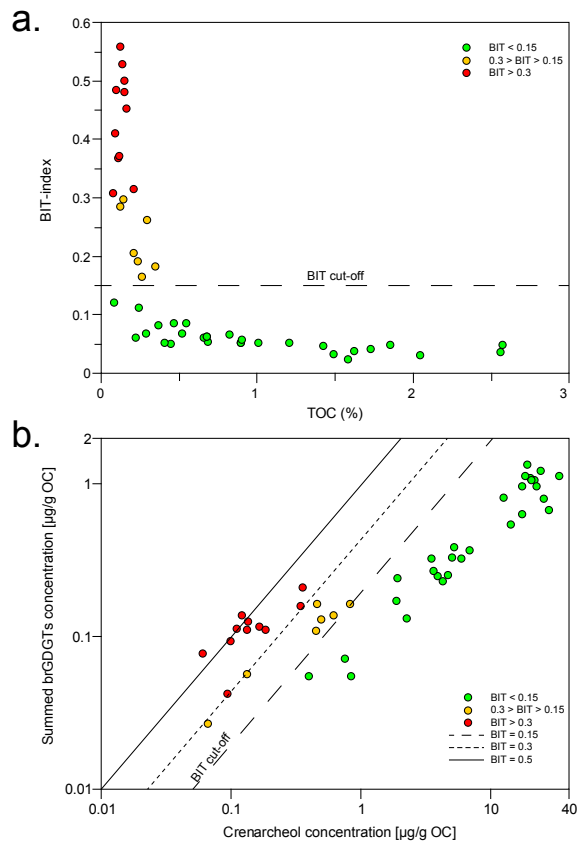
Figure 5. (a) Cross plot of summed brGDGTs (µg g^{-1} OC) vs. crenarcheol (µg g^{-1} OC) on a logarithmic axis. **(b)** Cross plot of BIT-index values vs. total organic carbon (TOC).

Figure 6. Geochemical and palynological results for the Cenomanian–Turonian transition of the Wunstorf core. Stratigraphy from Voigt et al. (2008). **(a)** $\delta^{13}C_{carb}$ (Voigt et al., 2008) and $\delta^{13}C_{org}$ (du Vivier et al., 2014; red). **(b)** Total organic carbon (TOC; black, this study; red, Hetzel et al., 2011). **(c)** TEX$_{86}$-values and TEX$_{86}^H$-based SST reconstruction (Kim et al., 2010) **(d)** Relative abundance (%) and absolute abundance in cysts per dry gram of sediment (cpg), of the dinocyst species *Cyclonephelium compactum- C. membraniphorum* complex, 'X' represents barren samples. **(e)**. Terrestrial vs. marine palynomorphs (T/M-ratio) and total pollen and spores in grains per dry gram of sediment (gpg), saccate gymnosperm pollen in dark green **(f)** Peridiniod vs. gonyaulacoid dinocysts (P/G-ratio). The grey zone indicates the OAE2 interval after Voigt et al. (2008). mbs = meters below surface.

Title Page

Abstract | Introduction

Conclusions | References

Tables | Figures

|◄ | ►|

◄ | ►

Back | Close

Full Screen / Esc

Printer-friendly Version

Interactive Discussion